



**HAL**  
open science

## Combining two optimized and affordable methods to assign chemoreceptors to a specific signal

Anne Boyeldieu, Amine Ali Chaouche, Vincent Méjean, Cécile Jourlin-Castelli

► **To cite this version:**

Anne Boyeldieu, Amine Ali Chaouche, Vincent Méjean, Cécile Jourlin-Castelli. Combining two optimized and affordable methods to assign chemoreceptors to a specific signal. *Analytical Biochemistry*, 2021, 620, pp.114139. 10.1016/j.ab.2021.114139 . hal-03195889

**HAL Id: hal-03195889**

**<https://hal.science/hal-03195889v1>**

Submitted on 10 Mar 2023

**HAL** is a multi-disciplinary open access archive for the deposit and dissemination of scientific research documents, whether they are published or not. The documents may come from teaching and research institutions in France or abroad, or from public or private research centers.

L'archive ouverte pluridisciplinaire **HAL**, est destinée au dépôt et à la diffusion de documents scientifiques de niveau recherche, publiés ou non, émanant des établissements d'enseignement et de recherche français ou étrangers, des laboratoires publics ou privés.



Distributed under a Creative Commons Attribution - NonCommercial 4.0 International License

1 **Combining two optimized and affordable methods to assign chemoreceptor(s) to a specific**  
2 **signal**

3

4 **Anne Boyeldieu<sup>a</sup>, Amine Ali Chaouche<sup>a</sup>, Vincent Méjean<sup>a</sup>, Cécile Jourlin-Castelli<sup>a\*</sup>**

5

6 Short title: Assigning chemoreceptor(s) to a ligand

7

8 <sup>a</sup>Aix Marseille Univ, CNRS, BIP UMR 7281, IMM, IM2B, Marseille, France

9

10 \*Corresponding author

11 Mailing address: Laboratoire de Bioénergétique et Ingénierie des Protéines (BIP-UMR7281), Institut  
12 de Microbiologie de la Méditerranée, Centre National de la Recherche Scientifique, 31 chemin  
13 Joseph Aiguier, CS 70071, 13402 Marseille cedex 09, France

14 Tel: 33 4 91 16 40 32

15 Fax: 33 4 91 16 40 97

16 E-mail: [jourlin@imm.cnrs.fr](mailto:jourlin@imm.cnrs.fr)

17

18

19 Subject Category : Special Topics

20 **Abstract**

21 Chemotaxis allows bacteria to detect specific compounds and move accordingly. This pathway  
22 involves signal detection by chemoreceptors (MCPs). Attributing a chemoreceptor to a ligand is  
23 difficult because there is a lot of redundancy in the MCPs that recognize a single ligand. We propose  
24 a methodology to define which chemoreceptors bind a given ligand. First, an MCP is overproduced to  
25 increase sensitivity to the ligand(s) it recognizes, thus promoting accumulation of cells around an  
26 agarose plug containing a low attractant concentration. Second, the ligand-binding domain (LBD) of  
27 the chemoreceptor is fused to maltose-binding protein (MBP), which facilitates purification and  
28 provides a control for a thermal shift assay (TSA). An increase in the melting temperature of the LBD  
29 in the presence of the ligand indicates that the chemoreceptor directly binds it. We showed that  
30 overexpression of two *Shewanella oneidensis* chemoreceptors (SO\_0987 and SO\_1056) promoted  
31 swimming toward an agarose plug containing a low concentration of chromate. The LBD of each of  
32 the two chemoreceptors was fused to MBP. A TSA revealed that only the LBD from SO\_1056 had its  
33 melting temperature increased by chromate. In conclusion, we describe an efficient approach to define  
34 chemoreceptor-ligand pairs before undertaking more-sophisticated biochemical and structural studies.

35  
36 **Keywords:** Bacterial chemotaxis; Signal detection; Methyl-accepting Chemotaxis Protein; Thermal  
37 Shift Assay; Agarose-in-plug bridge assay; MBP chimeric proteins.

38

## 39 **1. Introduction**

40 Bacteria encounter changing environments to which they adapt via a variety of mechanisms. In  
41 addition to adaptation through the regulation of gene expression, bacteria also control their movement  
42 within their environment using a mechanism called chemotaxis [1,2]. Upon detection of signal  
43 molecules called chemoeffectors, cells modulate their swimming behavior to move toward attractants  
44 or away from repellents. Chemotaxis is governed by a complex regulatory system composed of various  
45 Che proteins [3]. The well-conserved CheA-CheY histidine-kinase/response-regulator pair, which  
46 engage in a phosphorylation cascade, directly controls the rotational direction of the flagellum, which  
47 propels the bacterium. The first step in chemotaxis is the detection of chemoeffectors by specific  
48 chemoreceptor proteins called MCPs (Methyl-accepting Chemotaxis Proteins) [2,4]. The binding of  
49 chemoeffectors to MCPs then affects the phosphorylation cascade involving CheA-CheY, and  
50 consequently, bacterial movement.

51 Bacterial genomic analysis has revealed a large number of MCP-encoding genes, with some bacteria  
52 containing more than 80 [5]. Chemoreceptors are characterized by the presence of a highly conserved  
53 signaling domain within their cytoplasmic region. However, they also contain additional domains.  
54 Chemoreceptors can be classified according to the number of helical heptads that are contained within  
55 their signaling domain [5,6]. They can also be classified based on their topologies and the type of  
56 ligand-binding domain (LBD) they contain [4,7]. Cache, 4HB and PAS-containing domains are among  
57 the most common types of LBDs. The first described Cache domains were involved in small-molecule  
58 recognition [8]. Today, a large superfamily of different types of single and double Cache domains has  
59 been documented, and some ligands, such as amino acids, polyamines, carboxylic acids, sugars and  
60 hydrocarbons have been identified [9–11]. The 4HB (four-helix bundle) domain, which is widespread  
61 in signal transduction systems, has been shown to bind ligands such as amino, aromatic and carboxylic  
62 acids directly [10,12]. PAS domains, which are exclusively present in the cytoplasm, allow signal  
63 detection via direct binding to small molecules, including divalent cations or carboxylic acids. PAS-  
64 domain interactions can also be mediated by the presence of cofactors (heme b or c, FAD, FMN) for  
65 detection of signals such as oxygen or redox potential [13].

66 *Escherichia coli*, which has been a model for bacterial chemotaxis for many years, possesses only five  
67 chemoreceptors, all of which have been well characterized [14]. Four *E. coli* chemoreceptors contain  
68 a 4HB domain (Tar, Tsr, Trg and Tap), while one possesses a FAD-containing PAS domain (Aer). *E.*  
69 *coli* is able to respond chemotactically to various signals, including amino acids, sugars, dipeptides,  
70 quorum-sensing signals, pH and redox potential. Some signals are directly detected by the  
71 chemoreceptors, while the detection of others requires auxiliary proteins. For example, the Tar

72 chemoreceptor detects aspartate by direct binding to the Tar LBD and recognizes maltose via the  
73 maltose-binding protein (MBP).

74 Many bacteria have far more chemoreceptors than *E. coli*, especially bacteria that typically encounter  
75 changing environmental conditions [15]. For example, several species of the *Pseudomonas* genus  
76 contain more than 20 chemoreceptors. Aside from classical ligands (amino acids, carboxylic acids,  
77 sugars), some Pseudomonads use specific chemoreceptors to detect atypical molecules such as toluene,  
78 aromatic hydrocarbons and naphthalene [16]. *Shewanella oneidensis*, an aquatic bacterium, possesses  
79 27 chemoreceptors. It is chemotactically attracted to various respiratory substrates (oxygen, nitrate,  
80 fumarate, TMAO), but, more surprisingly, it is also attracted to chromate, a toxic compound [17–19].  
81 While five chemoreceptors have been shown to be involved in responses to respiratory substrates [18],  
82 the chemoreceptor(s) responsible for detecting chromate remain(s) unknown.

83 Despite the fact that the number of characterized LBDs has increased over last few years, it remains  
84 challenging to assign a ligand to a chemoreceptor, and vice versa. This is especially true because MCPs  
85 containing LBDs of the same type may detect many different ligands. Additionally, the same ligand  
86 may be detected by MCPs with different types of LBD. One strategy corresponds to the  
87 characterization of chemoreceptors one by one, testing their capacity to bind molecules from various  
88 libraries *in vitro* [20,21]. This strategy allows the identification of one or several compounds capable  
89 of binding a chemoreceptor. However, compounds identified in this way are not necessarily  
90 chemoeffectors, since the method does not assess their capacity to elicit a chemotactic response.  
91 Nevertheless, this strategy can be helpful when no chemoeffector has been identified within the  
92 organism studied, since the identification of chemoreceptor ligands has the potential to inform about  
93 the nature of compounds to which an organism may respond. However, a chemoeffector detected by a  
94 specific chemoreceptor can be missed using this strategy, because many chemoreceptors detect signals  
95 indirectly, for instance via interactions with periplasmic ligand-binding proteins.

96 Use of a different strategy based on gene deletions is possible when compounds are known to elicit  
97 chemotactic behavior for a given bacterium since, in this scenario, one must determine which  
98 chemoreceptor(s) is involved in the detection of a specific compound [22]. As mentioned above, this  
99 too may be complicated by the fact that bacteria usually possess many chemoreceptors and more than  
100 one chemoreceptor is often capable of detecting the same ligand. Here, we propose an easy and  
101 inexpensive strategy combining optimized versions of *in vivo* and *in vitro* experiments to determine  
102 which chemoreceptor(s) is/are involved in the direct recognition of a ligand via their LBD.

103

## 104 **2. Materials and Methods**

### 105 **2.1 Strains.**

106 The wild-type *S. oneidensis* strain used in this study was MR1-R [23]. All strains were routinely grown  
107 at 28°C (*S. oneidensis* strains) or 37°C (*E. coli* strains) in lysogeny broth (LB) medium. When  
108 necessary, chloramphenicol (25 µg/ml), rifampicin (10 µg/ml) or ampicillin (50 µg/ml) was added.  
109 The concentration of arabinose used for inducing expression of plasmid-borne genes was 0.2%.

110

### 111 **2.2 Construction of double-deletion mutant.**

112 The  $\Delta$ SO0987 $\Delta$ SO1056 mutant strain was constructed by sequential deletion of the *so\_0987* and  
113 *so\_1056* genes from the genome of the wild-type strain. This deletion mutant was constructed by  
114 homologous recombination as described previously [18]. Briefly, 500 bp flanking regions downstream  
115 and upstream of the gene to be deleted were cloned into the suicide vector pKNG101. The resulting  
116 plasmid was introduced into the *E. coli* strain CC118 $\lambda$ pir [24] and transferred into the appropriate *S.*  
117 *oneidensis* strain by conjugation using the *E. coli* helper strain 1047/pRK2013 [25]. The plasmid was  
118 integrated into the chromosome by a first recombination event and removed by a second recombination  
119 event in the presence of 6% sucrose. Deletions were confirmed using PCR and appropriate primers.

120

### 121 **2.3 Construction of plasmids.**

122 All plasmids used in this study are listed in Table 1. To construct pSO0987, pSO1056, pSO2240,  
123 pSO3282, pSO4053, pSO4454 and pSO4557, the coding sequences of the respective genes were  
124 amplified by PCR using *S. oneidensis* DNA as a template and primers containing appropriate  
125 restriction sites and an optimized Shine Dalgarno sequence. After digestion, PCR products were  
126 inserted into the pBAD33 vector. To construct pMAL-LBD-0987 and pMal-LBD-1056, the sequences  
127 encoding the LBD of SO\_0987 (Y30 to S200) and SO\_1056 (S29 to M278) were amplified by PCR  
128 using *S. oneidensis* DNA as a template and primers containing appropriate restriction sites. After  
129 digestion, PCR products were inserted into the pMAL-c2X vector. The sequences of all constructs  
130 were confirmed via DNA sequencing using appropriate primers.

131

132

133 **Table 1**

134 Plasmids used in this study

Plasmids	Descriptions	References
pBAD33	Vector containing pBAD promoter with the p15A origin of replication, Cm <sup>R</sup>	[26]
pSO0987	<i>so_0987</i> sequence cloned into pBAD33	This work
pSO1056	<i>so_1056</i> sequence cloned into pBAD33	This work
pSO2240	<i>so_2240</i> sequence cloned into pBAD33	This work
pSO3282	<i>so_3282</i> sequence cloned into pBAD33	This work
pSO4053	<i>so_4053</i> sequence cloned into pBAD33	This work
pSO4454	<i>so_4454</i> sequence cloned into pBAD33	This work
pSO4557	<i>so_4557</i> sequence cloned into pBAD33	This work
pMAL-c2X	Vector containing <i>ptac</i> promoter and the coding sequence of MBP, Amp <sup>R</sup>	New England Biolabs
pMAL-LBD-0987	Sequence coding for the ligand-binding domain of SO_0987 (Y30 to S200) cloned into pMAL-c2X	This work
pMAL-LBD-1056	Sequence coding for the ligand-binding domain of SO_1056 (S29 to M278) cloned into pMAL-c2X	This work
pKNG101	R6K-derived suicide plasmid containing Str <sup>R</sup> and <i>sacB</i>	[24]
pRK2013	RK2-Tra1 RK2-Mob1 Kan <sup>R</sup> <i>ori</i> ColE1	[25]

135

136

137

## 138 **2.4 Agarose-in-plug bridge assays.**

139 *2.4.1 Construction of bridge slide.* Microscope bridge slides were constructed as described previously  
140 [27]. Briefly, two square coverslips were placed on each side of a PETG slide. Four to eight agarose  
141 plugs per slide were made by pipetting 5 $\mu$ l preheated 2% low-melting agarose that contained the  
142 chemical to be tested onto the slide. Within a few seconds, a glass coverslip (24 mm  $\times$  60 mm) was  
143 placed over the slide. The bridge structure is maintained using a cyanoacrylate adhesive.

144

145 *2.4.2 Cell preparation and microscopic observation.* Cells were prepared as described in Armitano et  
146 al. [27], with slight modifications. Briefly, cells were grown overnight in LB medium under shaking  
147 conditions at 28°C. Cells were subsequently diluted in fresh LB medium at an OD<sub>600</sub> value of 0.05 and  
148 grown under shaking conditions until an OD<sub>600</sub> value of 0.7-0.8 was reached. Cells were then harvested  
149 by centrifugation (10 min at 3,500 rpm) and gently resuspended in LM medium (0.2 g/l yeast extract,  
150 0.1 g/l peptone, 10 mM HEPES (pH 7.4) and 10 mM NaHCO<sub>3</sub>) containing 20 mM lactate and 0.1%  
151 Tween-20 to produce an OD<sub>600</sub> of 0.2. After 30 min of static incubation at room temperature, 150  $\mu$ L  
152 of cell suspension was introduced within the microscope slide bridge. Photographs were taken at the  
153 edges of the plugs after 30 min with a 4X phase contrast objective. Strains containing pBAD33,  
154 pSO0987, pSO1056, pSO2240, pSO3282, pSO4053, pSO4454 or pSO4557 were grown overnight in  
155 the presence of chloramphenicol, and arabinose was subsequently added to induce gene expression.

156

## 157 **2.5 Expression and purification of MBP-LBD chimeric proteins.**

158 Recombinant MBP-tagged proteins, MBP-LBD<sub>0987</sub> and MBP-LBD<sub>1056</sub>, were produced from the *E. coli*  
159 C600 strain [28] that contained a pMAL-LBD-0987 or pMAL-LBD-1056 plasmid, respectively. The  
160 strains were grown aerobically at 37°C in LB medium. At OD<sub>600</sub> = 0.5, overproduction of proteins was  
161 induced with 0.3 mM isopropyl  $\beta$ -D-thiogalactopyranoside (IPTG). After 3 h at 37°C, cells were  
162 collected by centrifugation and resuspended in 20 mM Tris-HCl (pH 7.4), 200 mM NaCl, and 1 mM  
163 EDTA. Thereafter, they were lysed using a French press and centrifuged at 11,000 rpm for 20 min at  
164 4°C. After an ultracentrifugation step at 45,000 rpm for 1 h at 4°C, the supernatant was loaded onto an  
165 amylose high-flow resin (New England Biolabs), and proteins were purified according to the  
166 manufacturer's protocol. Purified proteins were loaded onto a PD-10 desalting column (GE  
167 Healthcare) and recovered in 20 mM Tris-HCl (pH 7.4) containing 100 mM NaCl. Protein



168 concentrations were determined using a Bradford assay (Bio-Rad). Purified proteins were store at  
169 - 80°C in 20 mM Tris-HCl (pH 7.4), 100 mM NaCl and 10% glycerol.

170

## 171 **2.6 Thermal shift assays.**

172 TSAs were carried out using purified proteins in 20 mM Tris-HCl (pH 7.4), 100 mM NaCl and 10 %  
173 glycerol in a total volume of 20  $\mu$ L, as described previously [29]. Briefly, either MBP-LBD<sub>0987</sub> (11.2  
174  $\mu$ M) or MBP-LBD<sub>1056</sub> (7.8  $\mu$ M) was incubated in the presence of 10X SYPRO Orange (Sigma Life  
175 Science) with or without potassium chromate (1 mM and 10 mM) and maltose (10 mM). Samples were  
176 then heated from 10 to 90°C at a scan rate of 0.5°C per 30 s using a BioRad CFX96 Touch Real Time  
177 PCR instrument. Protein unfolding curves were monitored by detecting changes in SYPRO Orange  
178 fluorescence. Melting temperatures were determined from first derivative values of raw fluorescence  
179 data using BioRad CFX Manager 3.1 software.

180

## 181 **3. Results and Discussion**

### 182 **3.1 Scientific rationale of the experimental strategy.**

183 Various techniques have been described to test the chemotactic abilities of bacteria. Among these, the  
184 agarose-in-plug bridge assay has been successfully used to study the behavior of different bacterial  
185 species [16,27,30–34]. Using this approach, the chemical to be tested is included in an agarose drop  
186 and placed on a microscope slide. A bacterial suspension is then injected in the area surrounding the  
187 agarose. If the chemical is an attractant, its diffusion into the bacterial suspension will cause cells to  
188 move toward the plug, which produces a microscopically observable bright ring of cells. One can then  
189 compare the behavior of a wild-type strain to that of mutants that harbor an MCP-deletion.

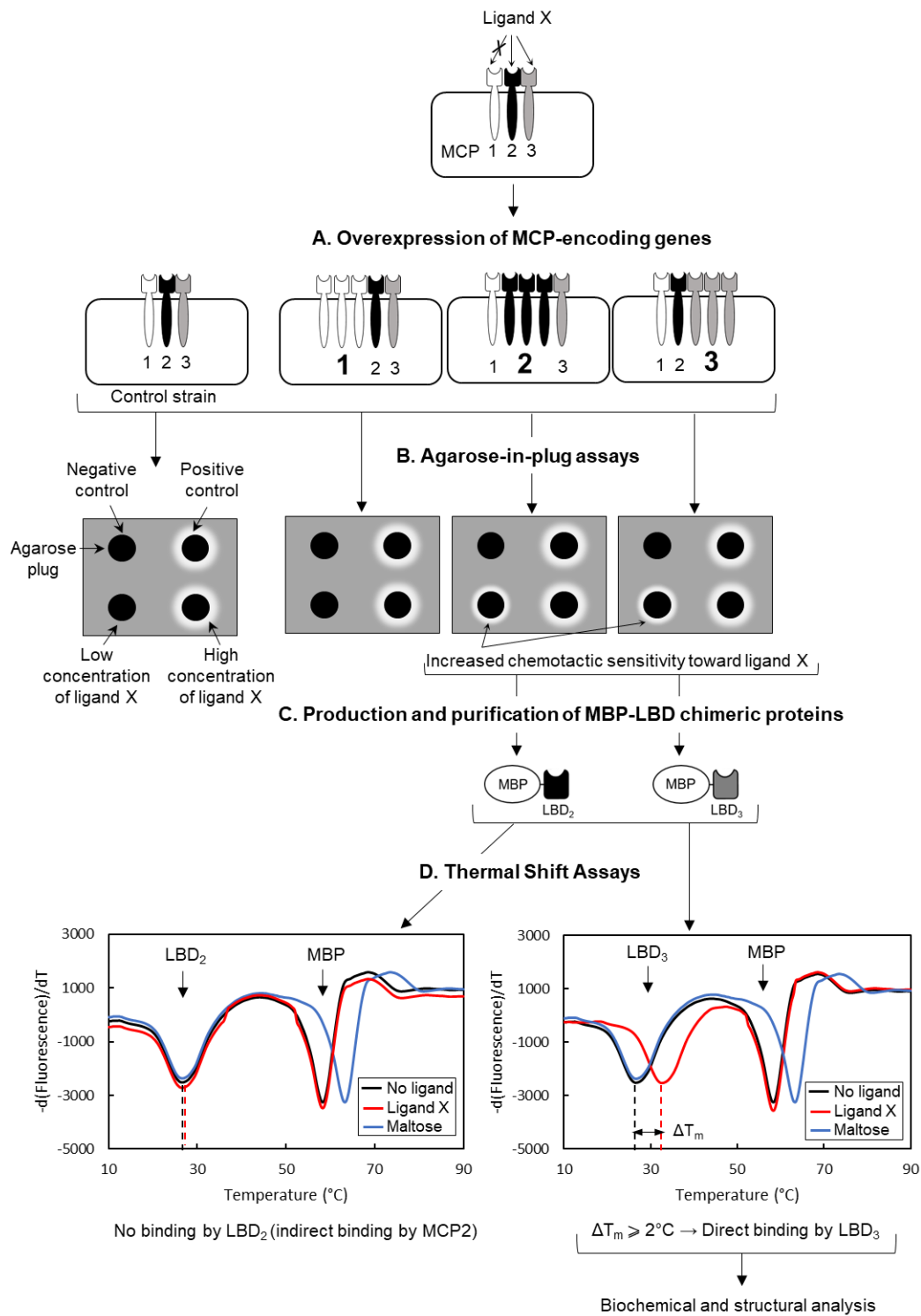
190 However, because signal-detection redundancy occurs, in which several MCPs bind the same ligand,  
191 the behavior of a single MCP-deletion mutant may not be distinguishable from that of its wild-type  
192 counterpart. Moreover, a gene-deletion analysis is not an easy task for bacteria that contain many  
193 chemoreceptor-encoding genes. To overcome this pitfall, we propose the use of a reverse  
194 methodology. Using this experimental rationale, instead of deleting an MCP-encoding gene in order  
195 to observe a reduced chemotactic response after exposure to a specific ligand, we propose cloning and  
196 overexpressing MCP-encoding genes in a wild-type strain. As the relative expression level of a  
197 chemoreceptor defines the sensitivity of response it mediates [35], the capacity of the resulting strains

198 to detect and respond to a concentration below that to which a control strain containing an empty vector  
199 is able to respond will be checked (Fig. 1A and B).

200 The chemoreceptor(s) identified by this approach will be tested *in vitro* using a simple thermal shift  
201 assay (TSA) to determine whether or not the detection of chemoattractant occurs via direct binding of  
202 the ligand to the chemoreceptor(s). Since the heterologous expression of entire chemoreceptors or of  
203 their LBDs in *Escherichia coli* could result in the formation of insoluble proteins that form inclusion  
204 bodies [36], we suggest that LBDs should be produced as chimeric proteins fused to MBP. Fusion to  
205 MBP has previously been shown to facilitate the solubilization of proteins that otherwise formed  
206 inclusion bodies (Fig. 1C) [37,38]. This strategy is an alternative to the recovery of proteins from  
207 inclusion bodies, which requires subsequently refolding and purification [36]. Interaction between a  
208 chimeric protein and ligand can then be assessed using a TSA [39]. This rapid and inexpensive  
209 technique is easy to set up and requires only a thermocycler, which is commonly found in microbiology  
210 laboratories. Moreover, it requires only low concentrations of proteins and can be performed in 96-  
211 well microplates, unlike isothermal titration calorimetry (ITC), which is a direct binding test  
212 commonly used to confirm ligand-protein interactions.

213 TSA requires proteins to be subjected to thermal denaturation in the presence of a dye (SYPRO  
214 Orange), which is fluorescently active when bound to hydrophobic domains of proteins exposed by  
215 thermal unfolding. Usually, ligand binding to a protein increases its thermal stability, which produces  
216 a detectable shift to a higher melting temperature (Fig. 1D). Moreover, TSA was previously proved to  
217 be a suitable technique for ligand-chemoreceptor interaction screening [20,21,40,41]. Adding MBP to  
218 form a chimeric protein provides an additional advantage, since MBP is able to function as an internal  
219 control whose denaturation profile should only be affected by maltose, its natural ligand. Below, we  
220 describe how this combined strategy was used to characterize chemoreceptor(s) involved in the  
221 detection of chromate, an attractant peculiar to *S. oneidensis*.

222



223

224 **Figure 1. A scheme outlining the strategy used to identify chemoreceptors (MCPs) involved in specific ligand**  
 225 **recognition.** A) Each gene encoding an MCP to be tested was overexpressed in a wild-type background. B) Agarose-in  
 226 plug assays were used to test the chemotactic behavior of each MCP-overexpressing strain toward ligand X. MCPs whose  
 227 overproduction enhances the chemotactic sensitivity of the wild-type strain, as indicated by a bright ring of cells around a  
 228 plug containing a low concentration of ligand X, are selected as candidates for ligand X recognition. C) The ligand-binding  
 229 domains (LBD) of the selected MCPs are fused to maltose-binding protein (MBP). The resulting MBP-LBD fusions are  
 230 overproduced and purified, taking advantage of the ability of MBP to bind to amylose. D) Interactions between MBP-LBD

231 fusions and ligand X are tested using TSA. Curves of the first derivative of fluorescence emission with respect to  
232 temperature should contain two negative peaks that corresponded either to the MBP or LBD moiety of each chimeric  
233 protein. Maltose is used to identify the peak that corresponds to MBP. The two peaks allow us to determine the melting  
234 temperature ( $T_m$ ) of each moiety of the chimeric protein in the absence and presence of ligand X. When the addition of  
235 ligand X does not modify the  $T_m$  of the LBD, ligand X probably does not bind directly to the LBD. A  $T_m$  shift for the LBD  
236 in the presence of ligand X ( $\Delta T_m \geq 2^\circ\text{C}$ ) indicates that the LBD binds ligand X directly. The LBD-ligand X interaction  
237 can then be further characterized with other methods.

238

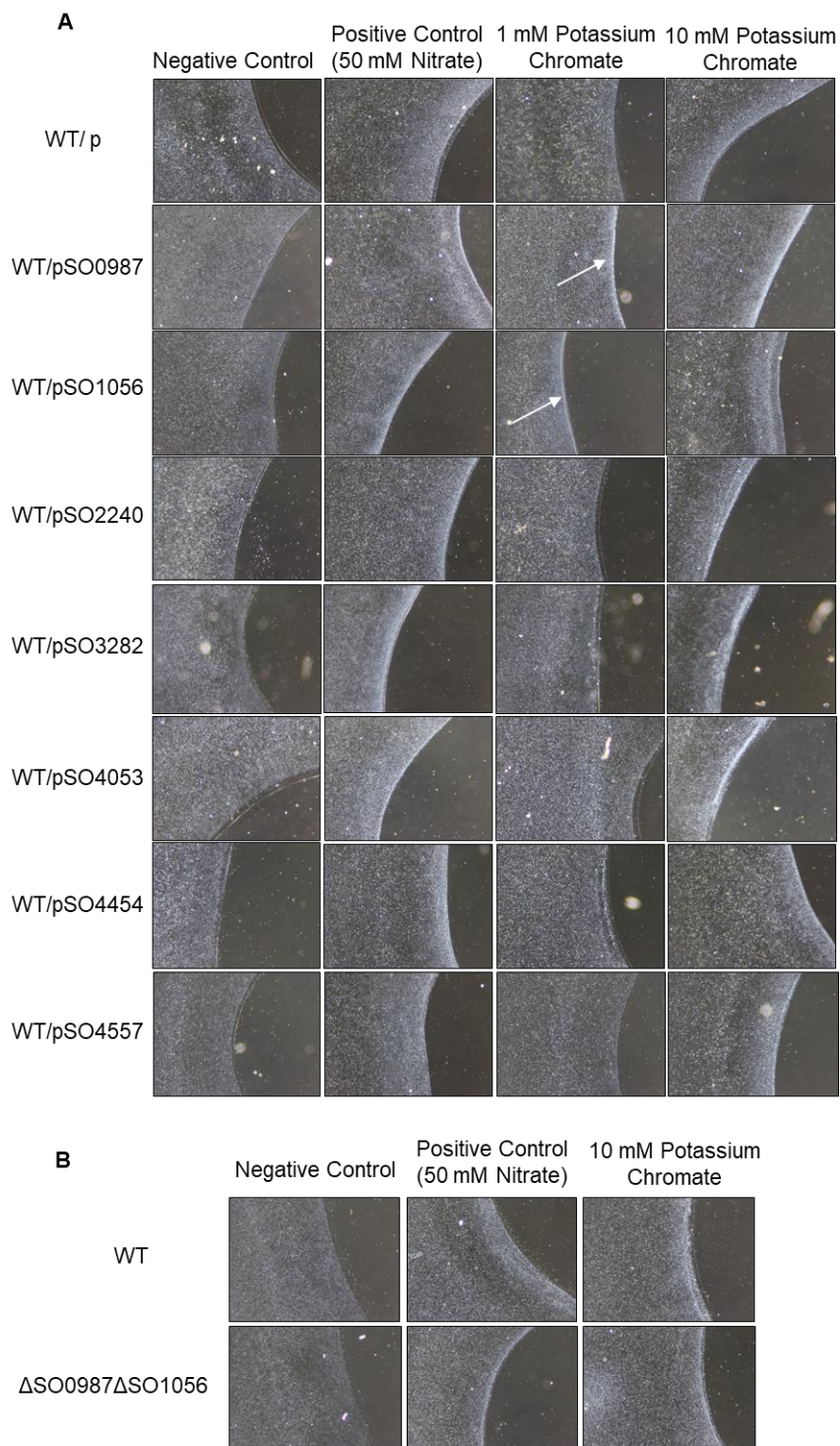
### 239 **3.2 Combining the overexpression of chemoreceptor-encoding genes with an agarose-in-plug** 240 **bridge assay enabled the identification of two chemoreceptors involved in the chemotactic** 241 **response to chromate.**

242 *S. oneidensis* is attracted to chromate, a toxic metal to which it is resistant [19]. To the best of our  
243 knowledge, this is the only example of bacterial chemotaxis toward chromate. Therefore, no specific  
244 motif for chromate binding has been previously described. Recently, we described an efflux pump,  
245 ChrA<sub>SO</sub>, involved in *S. oneidensis* chromate resistance [42]. A gene (*so\_0987*) encoding a  
246 chemoreceptor was identified immediately downstream and in the same orientation as the *chrA<sub>SO</sub>*  
247 (*so\_0986*) gene. Apart from its location, the *so\_0987* gene drew our attention because it encodes a  
248 chemoreceptor with a Cache domain in its LBD. Since Cache domains are capable of binding small  
249 molecules, we decided to test not only SO\_0987 but also other Cache-containing chemoreceptors for  
250 their ability to detect chromate [8]. The *S. oneidensis* genome is predicted to encode the following  
251 Cache-domain containing chemoreceptors: SO\_0987 and SO\_2240 (sCache2); SO\_1056, SO\_1278,  
252 SO\_4454, SO\_4557 and SO\_4466 (dCache1); SO\_4053 (dCache3) and SO\_3282 (Cache3-Cache2)  
253 [5]. Except for SO\_1278 and SO\_4466, which were associated with lowest Cache domain prediction  
254 E-values, all genes encoding Cache-containing chemoreceptors were independently cloned under the  
255 control of an arabinose-inducible promoter. The resulting plasmids were introduced into the wild-type  
256 *S. oneidensis* reference strain (MR1-R), and chemotactic behaviors of the strains were tested via the  
257 agarose-in-plug bridge assay.

258 As shown in Figure 2A, the wild-type strain that contained an empty vector was attracted to nitrate  
259 (used as a control) and also to chromate when it was present at 10 mM in the plug, as indicated by the  
260 presence of a bright ring of cells close to the plug. However, when only 1 mM chromate was added to  
261 the plug, it did not attract wild-type bacteria. Among the seven chemoreceptor genes tested, the  
262 overexpression of only two (*so\_0987* and *so\_1056*) resulted in a bright ring of cells around the plug  
263 containing 1 mM chromate; attraction to nitrate remained unchanged (Fig. 2A). These results indicate

264 that the cells overexpressing either *so\_0987* or *so\_1056* are attracted to chromate with a higher  
265 sensitivity than the control strain.

266 In addition to these two chemoreceptors, likely others are also involved in the detection of chromate,  
267 as a strain containing deletions of *so\_0987* and *so\_1056* was still attracted to chromate (Fig. 2B).



268

269 **Figure 2. Agarose-in-*plug* bridge assays to identify dedicated chemoreceptors.** A) Agarose-in-*plug* bridge assays of a  
270 wild-type (WT) *S. oneidensis* strain containing either an empty vector (p) or one of the seven plasmids bearing Cache-

271 containing MCP-encoding genes (pSO0987, pSO1056, pSO2240, pSO3282, pSO4053, pSO4454 or pSO4557) are shown.  
272 B) Agarose-in-plug bridge assays of wild-type (WT) and  $\Delta$ SO0987 $\Delta$ SO1056 strains are shown. Cells were grown in LB  
273 containing 0.2% arabinose under shaking conditions until an OD<sub>600</sub> of 0.7-0.8 was reached. Cells were then harvested by  
274 centrifugation and resuspended in LM medium containing lactate and Tween-20. The chemotactic behaviors of the strains  
275 toward a plug that contained either water (negative control), 50 mM sodium nitrate (positive control), or 1 mM or 10 mM  
276 potassium chromate were tested using an agarose-in-plug bridge assay. Photographs were taken at the edges of the plug  
277 after 30 min of incubation (4 $\times$  magnification). White arrows indicate the accumulation of cells around a plug containing a  
278 low concentration of potassium chromate (A). All pictures are representative of three independent experiments.

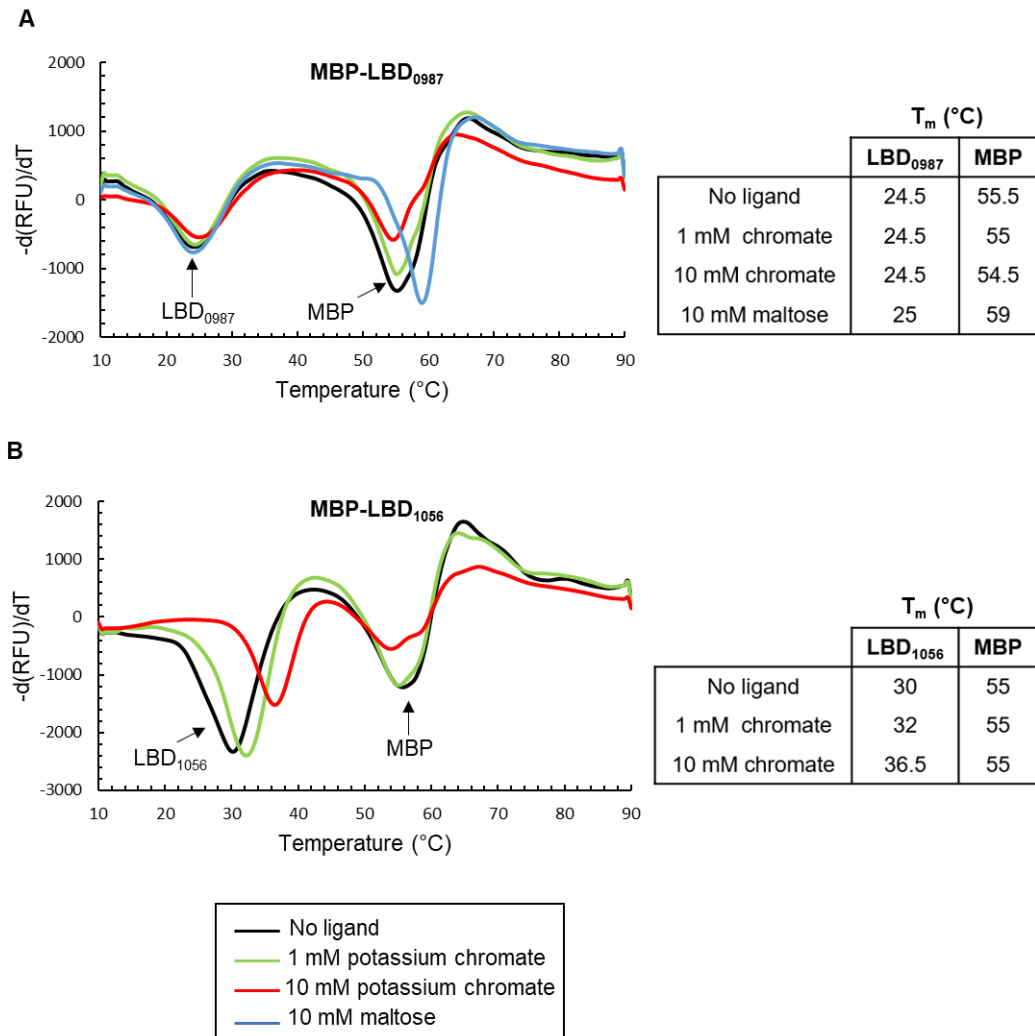
279

### 280 **3.3 The LBD of one of the two identified chemoreceptors directly binds chromate.**

281 To test whether the detection of chromate by the two chemoreceptors is direct, we performed TSAs  
282 using purified proteins. The SO\_0987 and SO\_1056 proteins are predicted to share a similar topology,  
283 with two transmembrane segments delimiting the LBD. Each LBD is predicted to be periplasmic and  
284 contains a Cache domain. Therefore, we cloned the region encoding the LBD of each chemoreceptor  
285 in frame with an MBP-encoding gene. The gene fusions were placed under the control of the IPTG-  
286 inducible *ptac* promoter, which allowed their overexpression. The two chimeric MBP-LBD proteins  
287 proved to be soluble when overproduced. Overproduction of the corresponding Strep-tagged LBDs  
288 resulted in insoluble proteins that were found in inclusion bodies.

289 The two chimeric MBP-LBD proteins were subsequently purified using an amylose resin column. The  
290 two purified proteins were then submitted to thermal denaturation in the presence of SYPRO Orange  
291 fluorescent dye. To determine the melting temperature ( $T_m$ ), the first derivatives of melt curves are  
292 shown (Fig. 3). Similar curves displaying two peaks were observed for each chimeric protein in the  
293 absence of ligand (Fig. 3A and B; black curves). We assumed that each moiety of the chimeric protein  
294 is capable of folding independently, and thus reacts differently to thermal denaturation.

295 To assign each peak to a specific moiety of the chimeric protein, we submitted the MBP-LBD<sub>0987</sub>  
296 protein to thermal denaturation in the presence of maltose, the ligand of MBP. Only the second peak  
297 of the melt curve of the chimeric protein shifted in response to the presence of maltose, indicating that  
298 this peak corresponded to the MBP moiety (Fig. 3A, blue curve). This strongly suggested that the first  
299 peak was associated with the LBD moiety of the chimeric protein.



300

301

302 **Figure 3. Thermal shift assays with MBP-LBD<sub>0987</sub> and MBP-LBD<sub>1056</sub> in the absence and presence of potassium**  
 303 **chromate and maltose.** A) Thermal shift assays with MBP-LBD<sub>0987</sub> in the absence or in the presence of 1 or 10 mM  
 304 potassium chromate, or 10 mM maltose, are shown. B) Thermal shift assays with MBP-LBD<sub>1056</sub> in the absence or in  
 305 presence of 1mM or 10 mM potassium chromate are shown. Graphs represent the first derivative of the fluorescence  
 306 emission (-d(RFU)/dT, RFU: Raw Fluorescence Unit) as a function of temperature. The melting temperatures ( $T_m$ ) of each  
 307 peak are listed in the tables to the right of each graph. Each graph is colored according to the tested ligand, as indicated.  
 308 All graphs represent the results of three independent experiments.

309

310 We then performed TSAs to test chromate binding to both chimeric proteins. For MBP-LBD<sub>0987</sub>,  
 311 neither 1 mM nor 10 mM chromate shifted the melt curve, and the  $T_m$  calculated for each moiety was  
 312 not significantly modified (Fig. 3A). In contrast, for MBP-LBD<sub>1056</sub>, chromate modified its melting  
 313 curve. Only the peak assigned to the LBD<sub>1056</sub> moiety was altered, whereas the peak corresponding to  
 314 MBP remained unaffected (Fig. 3B), signifying that the  $T_m$  associated with the MBP moiety remained

315 unchanged by chromate. The  $T_m$  that corresponded to the LBD<sub>1056</sub> moiety increased significantly (2°C  
316 and 6.5°C in the presence of 1 mM and 10 mM chromate, respectively). A  $T_m$  shift of 2°C or more is  
317 considered significant and is a strong indicator of ligand binding [11,21,40,41].

318 Of the two chemoreceptors we identified as being involved in the chemotactic response to chromate,  
319 TSA indicated that one (SO\_1056) directly binds chromate via its Cache-containing LBD. For the  
320 second chemoreceptor (SO\_0987), no evidence of direct binding of chromate to the LBD was obtained.  
321 This finding indicates that either the chemoreceptor binds chromate via a different region of the  
322 protein, that chromate detection is indirect and requires an additional protein, or that for some unknown  
323 reason chromate binding to the LBD does not cause a significant shift in the melting temperature.

324

## 325 **4. Conclusion**

326 We previously developed a high-throughput technique to identify novel molecules that elicit a  
327 chemotactic response in bacteria [19]. Here, we propose a combination of efficient and simple  
328 protocols that can be used to assign chemotaxis-promoting compounds to chemoreceptors that bind  
329 their ligands directly. This approach can easily be scaled-up to perform high-throughput screening of  
330 chemoreceptors for a given ligand. As this is only a first step towards understanding signal detection,  
331 further characterization of the identified chemoreceptors must later be performed using more thorough  
332 biochemical techniques such as microscale thermophoresis, isothermal titration calorimetry, and  
333 structural analysis. The same approach could be used to identify the precise ligand-binding region after  
334 random mutagenesis of an LBD. Finally, these combined methods should be useful for biotechnology  
335 engineering, for example to design tools to detect pollutants.

336

## 337 **Acknowledgments**

338 We thank Marianne Ilbert, Amel Latifi and Baptiste Roumezi for their scientific and technical advices.  
339 We also thank Yann Denis from the Transcriptomic facility (IMM) for technical advices concerning  
340 TSAs. We thank all members of the group for their helpful discussions. We are also grateful to an  
341 anonymous reviewer whose suggestions helped improve and clarify this manuscript.

342

343 The authors acknowledge the funding from the Centre National de la Recherche Scientifique  
344 (www.cnrs.fr), Aix-Marseille Université (www.univ-amu.fr) and HTS-BIO (www.htsbio.com, Grant



345 N°152 660). A. B. was supported by a MESR fellowship and by an ATER position (Aix-Marseille  
346 Université). The funders had no role in study design, data collection and interpretation, or the decision  
347 to submit the work for publication.

348 The manuscript has been professionally proofread (Proof-Reading-Service.com).

349

350 AB, VM and CJC designed research. AB, AAC and CJC performed experiments. AB, AAC, VM and  
351 CJC analyzed data. AB, VM and CJC wrote the manuscript.

352

353 The authors declare no conflict of interest.

354

## 355 **References**

- 356 [1] G.H. Wadhams, J.P. Armitage, Making sense of it all: bacterial chemotaxis, *Nat. Rev. Mol. Cell*  
357 *Biol.* 5 (2004) 1024–1037. <https://doi.org/10.1038/nrm1524>.
- 358 [2] S. Bi, V. Sourjik, Stimulus sensing and signal processing in bacterial chemotaxis, *Curr. Opin.*  
359 *Microbiol.* 45 (2018) 22–29. <https://doi.org/10.1016/j.mib.2018.02.002>.
- 360 [3] V. Sourjik, N.S. Wingreen, Responding to chemical gradients: bacterial chemotaxis, *Curr. Opin.*  
361 *Cell Biol.* 24 (2012) 262–268. <https://doi.org/10.1016/j.ceb.2011.11.008>.
- 362 [4] A.I.M. Salah Ud-Din, A. Roujeinikova, Methyl-accepting chemotaxis proteins: a core sensing  
363 element in prokaryotes and archaea, *Cell. Mol. Life Sci.* 74 (2017) 3293–3303.  
364 <https://doi.org/10.1007/s00018-017-2514-0>.
- 365 [5] V.M. Gumerov, D.R. Ortega, O. Adebali, L.E. Ulrich, I.B. Zhulin, MiST 3.0: an updated  
366 microbial signal transduction database with an emphasis on chemosensory systems, *Nucleic*  
367 *Acids Res.* 48 (2020) D459–D464. <https://doi.org/10.1093/nar/gkz988>.
- 368 [6] R.P. Alexander, I.B. Zhulin, Evolutionary genomics reveals conserved structural determinants of  
369 signaling and adaptation in microbial chemoreceptors, *Proc. Natl. Acad. Sci. U.S.A.* 104 (2007)  
370 2885–2890. <https://doi.org/10.1073/pnas.0609359104>.
- 371 [7] J. Lacal, C. García-Fontana, F. Muñoz-Martínez, J.-L. Ramos, T. Krell, Sensing of environmental  
372 signals: classification of chemoreceptors according to the size of their ligand binding regions,  
373 *Environ. Microbiol.* 12 (2010) 2873–2884. <https://doi.org/10.1111/j.1462-2920.2010.02325.x>.

- 374 [8] V. Anantharaman, L. Aravind, Cache - a signaling domain common to animal Ca(2+)-channel  
375 subunits and a class of prokaryotic chemotaxis receptors, Trends Biochem. Sci. 25 (2000) 535–  
376 537. [https://doi.org/10.1016/s0968-0004\(00\)01672-8](https://doi.org/10.1016/s0968-0004(00)01672-8).
- 377 [9] A.A. Upadhyay, A.D. Fleetwood, O. Adebali, R.D. Finn, I.B. Zhulin, Cache Domains That are  
378 Homologous to, but Different from PAS Domains Comprise the Largest Superfamily of  
379 Extracellular Sensors in Prokaryotes, PLoS Comput. Biol. 12 (2016) e1004862.  
380 <https://doi.org/10.1371/journal.pcbi.1004862>.
- 381 [10] Á. Ortega, I.B. Zhulin, T. Krell, Sensory Repertoire of Bacterial Chemoreceptors, Microbiol.  
382 Mol. Biol. Rev. 81 (2017). <https://doi.org/10.1128/MMBR.00033-17>.
- 383 [11] A.F. Gasperotti, M.K. Herrera Seitz, R.S. Balmaceda, L.M. Prosa, K. Jung, C.A. Studdert, Direct  
384 binding of benzoate derivatives to two chemoreceptors with Cache sensor domains in *Halomonas*  
385 *titanicae* KHS3, Mol Microbiol. (2020). <https://doi.org/10.1111/mmi.14630>. Epub ahead of print.  
386 PMID: 33098326.
- 387 [12] L.E. Ulrich, I.B. Zhulin, Four-helix bundle: a ubiquitous sensory module in prokaryotic signal  
388 transduction, Bioinformatics. 21 Suppl 3 (2005) iii45-48.  
389 <https://doi.org/10.1093/bioinformatics/bti1204>.
- 390 [13] J.T. Henry, S. Crosson, Ligand-binding PAS domains in a genomic, cellular, and structural  
391 context, Annu. Rev. Microbiol. 65 (2011) 261–286. [https://doi.org/10.1146/annurev-micro-](https://doi.org/10.1146/annurev-micro-121809-151631)  
392 [121809-151631](https://doi.org/10.1146/annurev-micro-121809-151631).
- 393 [14] J.S. Parkinson, G.L. Hazelbauer, J.J. Falke, Signaling and sensory adaptation in *Escherichia coli*  
394 chemoreceptors: 2015 update, Trends Microbiol. 23 (2015) 257–266.  
395 <https://doi.org/10.1016/j.tim.2015.03.003>.
- 396 [15] L.D. Miller, M.H. Russell, G. Alexandre, Diversity in bacterial chemotactic responses and niche  
397 adaptation, Adv. Appl. Microbiol. 66 (2009) 53–75. [https://doi.org/10.1016/S0065-](https://doi.org/10.1016/S0065-2164(08)00803-4)  
398 [2164\(08\)00803-4](https://doi.org/10.1016/S0065-2164(08)00803-4).
- 399 [16] J. Lacal, F. Muñoz-Martínez, J.-A. Reyes-Darías, E. Duque, M. Matilla, A. Segura, J.-J.O. Calvo,  
400 C. Jiménez-Sánchez, T. Krell, J.L. Ramos, Bacterial chemotaxis towards aromatic hydrocarbons  
401 in *Pseudomonas*, Environ. Microbiol. 13 (2011) 1733–1744. [https://doi.org/10.1111/j.1462-](https://doi.org/10.1111/j.1462-2920.2011.02493.x)  
402 [2920.2011.02493.x](https://doi.org/10.1111/j.1462-2920.2011.02493.x).
- 403 [17] S. Bencharit, M.J. Ward, Chemotactic responses to metals and anaerobic electron acceptors in  
404 *Shewanella oneidensis* MR-1, J. Bacteriol. 187 (2005) 5049–5053.  
405 <https://doi.org/10.1128/JB.187.14.5049-5053.2005>.

- 406 [18] C. Baraquet, L. Théraulaz, C. Iobbi-Nivol, V. Méjean, C. Jourlin-Castelli, Unexpected  
407 chemoreceptors mediate energy taxis towards electron acceptors in *Shewanella oneidensis*, Mol.  
408 Microbiol. 73 (2009) 278–290. <https://doi.org/10.1111/j.1365-2958.2009.06770.x>.
- 409 [19] J. Armitano, C. Baraquet, V. Michotey, V. Méjean, C. Jourlin-Castelli, The chemical-in- $\mu$ well: a  
410 high-throughput technique for identifying solutes eliciting a chemotactic response in motile  
411 bacteria, Res. Microbiol. 162 (2011) 934–938. <https://doi.org/10.1016/j.resmic.2011.03.001>.
- 412 [20] M.K.G. Ehrhardt, S.L. Warring, M.L. Gerth, Screening Chemoreceptor-Ligand Interactions by  
413 High-Throughput Thermal-Shift Assays, Methods Mol. Biol. 1729 (2018) 281–290.  
414 [https://doi.org/10.1007/978-1-4939-7577-8\\_22](https://doi.org/10.1007/978-1-4939-7577-8_22).
- 415 [21] M. Fernández, Á. Ortega, M. Rico-Jiménez, D. Martín-Mora, A. Daddaoua, M.A. Matilla, T.  
416 Krell, High-Throughput Screening to Identify Chemoreceptor Ligands, Methods Mol. Biol. 1729  
417 (2018) 291–301. [https://doi.org/10.1007/978-1-4939-7577-8\\_23](https://doi.org/10.1007/978-1-4939-7577-8_23).
- 418 [22] A. Hida, T. Tajima, J. Kato, Two citrate chemoreceptors involved in chemotaxis to citrate and/or  
419 citrate-metal complexes in *Ralstonia pseudosolanacearum*, J. Biosci. Bioeng. 127 (2019) 169–  
420 175. <https://doi.org/10.1016/j.jbiosc.2018.07.014>.
- 421 [23] C. Bordi, C. Iobbi-Nivol, V. Méjean, J.-C. Patte, Effects of ISSo2 insertions in structural and  
422 regulatory genes of the trimethylamine oxide reductase of *Shewanella oneidensis*, J. Bacteriol.  
423 185 (2003) 2042–2045. <https://doi.org/10.1128/jb.185.6.2042-2045.2003>.
- 424 [24] M. Herrero, V. de Lorenzo, K.N. Timmis, Transposon vectors containing non-antibiotic  
425 resistance selection markers for cloning and stable chromosomal insertion of foreign genes in  
426 gram-negative bacteria., J. Bacteriol. 172 (1990) 6557–6567.  
427 <https://doi.org/10.1128/jb.172.11.6557-6567.1990>.
- 428 [25] D.H. Figurski, D.R. Helinski, Replication of an origin-containing derivative of plasmid RK2  
429 dependent on a plasmid function provided *in trans*, Proc. Natl. Acad. Sci. U.S.A. 76 (1979) 1648–  
430 1652. <https://doi.org/10.1073/pnas.76.4.1648>.
- 431 [26] L.M. Guzman, D. Belin, M.J. Carson, J. Beckwith, Tight regulation, modulation, and high-level  
432 expression by vectors containing the arabinose PBAD promoter, J. Bacteriol. 177 (1995) 4121–  
433 4130. <https://doi.org/10.1128/jb.177.14.4121-4130.1995>.
- 434 [27] J. Armitano, V. Méjean, C. Jourlin-Castelli, Aerotaxis governs floating biofilm formation in  
435 *Shewanella oneidensis*, Environ. Microbiol. 15 (2013) 3108–3118. <https://doi.org/10.1111/1462-2920.12158>.
- 436  
437 [28] R.K. Appleyard, Segregation of New Lysogenic Types during Growth of a Doubly Lysogenic  
438 Strain Derived from *Escherichia coli* K12, Genetics. 39 (1954) 440–452. <https://doi.org/>

- 439 [29] C. Gambari, A. Boyeldieu, J. Armitano, V. Méjean, C. Jourlin-Castelli, Control of pellicle  
440 biogenesis involves the diguanylate cyclases PdgA and PdgB, the c-di-GMP binding protein  
441 MxdA and the chemotaxis response regulator CheY3 in *Shewanella oneidensis*, *Environ.*  
442 *Microbiol.* 21 (2019) 81–97. <https://doi.org/10.1111/1462-2920.14424>.
- 443 [30] H.S. Yu, M. Alam, An agarose-in-plug bridge method to study chemotaxis in the Archaeon  
444 *Halobacterium salinarum*, *FEMS Microbiol. Lett.* 156 (1997) 265–269.  
445 <https://doi.org/10.1111/j.1574-6968.1997.tb12738.x>.
- 446 [31] G. Vardar, P. Barbieri, T.K. Wood, Chemotaxis of *Pseudomonas stutzeri* OX1 and *Burkholderia*  
447 *cepacia* G4 toward chlorinated ethenes, *Appl. Microbiol. Biotechnol.* 66 (2005) 696–701.  
448 <https://doi.org/10.1007/s00253-004-1685-4>.
- 449 [32] K.D. Collins, T.M. Andermann, J. Draper, L. Sanders, S.M. Williams, C. Araghi, K.M.  
450 Ottemann, The *Helicobacter pylori* CZB Cytoplasmic Chemoreceptor TlpD Forms an  
451 Autonomous Polar Chemotaxis Signaling Complex That Mediates a Tactic Response to  
452 Oxidative Stress, *J. Bacteriol.* 198 (2016) 1563–1575. <https://doi.org/10.1128/JB.00071-16>.
- 453 [33] V. Korolik, K.M. Ottemann, Two Spatial Chemotaxis Assays: The Nutrient-Depleted  
454 Chemotaxis Assay and the Agarose-Plug-Bridge Assay, *Methods Mol. Biol.* 1729 (2018) 23–31.  
455 [https://doi.org/10.1007/978-1-4939-7577-8\\_3](https://doi.org/10.1007/978-1-4939-7577-8_3).
- 456 [34] C. Roggo, E.E. Clerc, N. Hadadi, N. Carraro, R. Stocker, J.R. van der Meer, Heterologous  
457 Expression of *Pseudomonas putida* Methyl-Accepting Chemotaxis Proteins Yields *Escherichia*  
458 *coli* Cells Chemotactic to Aromatic Compounds, *Appl. Environ. Microbiol.* 84 (2018).  
459 <https://doi.org/10.1128/AEM.01362-18>.
- 460 [35] Y. Kalinin, S. Neumann, V. Sourjik, M. Wu, Responses of *Escherichia coli* bacteria to two  
461 opposing chemoattractant gradients depend on the chemoreceptor ratio, *J. Bacteriol.* 192 (2010)  
462 1796–1800. <https://doi.org/10.1128/JB.01507-09>.
- 463 [36] M.A. Machuca, A. Roujeinikova, Method for Efficient Refolding and Purification of  
464 Chemoreceptor Ligand Binding Domain, *J Vis Exp.* 130 (2017) 57092.  
465 <https://doi.org/10.3791/57092>.
- 466 [37] R.B. Kapust, D.S. Waugh, *Escherichia coli* maltose-binding protein is uncommonly effective at  
467 promoting the solubility of polypeptides to which it is fused, *Protein Sci.* 8 (1999) 1668–1674.  
468 <https://doi.org/10.1110/ps.8.8.1668>.
- 469 [38] S. Raran-Kurussi, D.S. Waugh, The ability to enhance the solubility of its fusion partners is an  
470 intrinsic property of maltose-binding protein but their folding is either spontaneous or chaperone-  
471 mediated, *PLoS ONE.* 7 (2012) e49589. <https://doi.org/10.1371/journal.pone.0049589>.

- 472 [39] F.H. Niesen, H. Berglund, M. Vedadi, The use of differential scanning fluorimetry to detect  
473 ligand interactions that promote protein stability, *Nat Protoc.* 2 (2007) 2212–2221.  
474 <https://doi.org/10.1038/nprot.2007.321>.
- 475 [40] D. Martín-Mora, A. Ortega, J.A. Reyes-Darias, V. García, D. López-Farfán, M.A. Matilla, T.  
476 Krell, Identification of a Chemoreceptor in *Pseudomonas aeruginosa* That Specifically Mediates  
477 Chemotaxis Toward  $\alpha$ -Ketoglutarate, *Front Microbiol.* 7 (2016) 1937.  
478 <https://doi.org/10.3389/fmicb.2016.01937>.
- 479 [41] J.L.O. McKellar, J.J. Minnell, M.L. Gerth, A high-throughput screen for ligand binding reveals  
480 the specificities of three amino acid chemoreceptors from *Pseudomonas syringae* pv. *actinidiae*,  
481 *Mol Microbiol.* 96 (2015) 694–707. <https://doi.org/10.1111/mmi.12964>.
- 482 [42] H. Baaziz, C. Gambari, A. Boyeldieu, A. Ali Chaouche, R. Alatou, V. Méjean, C. Jurlin-Castelli,  
483 M. Fons, ChrASO, the chromate efflux pump of *Shewanella oneidensis*, improves chromate  
484 survival and reduction, *PLoS ONE.* 12 (2017) e0188516.  
485 <https://doi.org/10.1371/journal.pone.0188516>.  
486  
487

